6558–6569 *Nucleic Acids Research, 2012, Vol. 40, No. 14* *Published online 9 April 2012*
doi:10.1093/nar/gks305

Rad51 presynaptic filament stabilization function of the mouse Swi5–Sfr1 heterodimeric complex

Shang-Pu Tsai[1], Guan-Chin Su[1], Sheng-Wei Lin[2], Chan-I. Chung[1], Xiaoyu Xue[3], Myun Hwa Dunlop[3], Yufuko Akamatsu[4], Maria Jasin[4], Patrick Sung[3] and Peter Chi[1,2,*]

[1]Institute of Biochemical Sciences, National Taiwan University, No. 1, Section 4, Roosevelt Road, Taipei, 10617, [2]Institute of Biological Chemistry, Academia Sinica, 128 Academia Road, Section 2, Nankang, Taipei 115, Taiwan, [3]Department of Molecular Biophysics and Biochemistry, Yale University School of Medicine, New Haven, CT 06520 and [4]Developmental Biology Program, Memorial Sloan-Kettering Cancer Center, New York, NY 10065, USA

Received February 14, 2012; Revised March 18, 2012; Accepted March 22, 2012

ABSTRACT

Homologous recombination (HR) represents a major error-free pathway to eliminate pre-carcinogenic chromosomal lesions. The DNA strand invasion reaction in HR is mediated by a helical filament of the Rad51 recombinase assembled on single-stranded DNA that is derived from the nucleolytic processing of the primary lesion. Recent studies have found that the human and mouse Swi5 and Sfr1 proteins form a complex that influences Rad51-mediated HR in cells. Here, we provide biophysical evidence that the mouse Swi5–Sfr1 complex has a 1:1 stoichiometry. Importantly, the Swi5–Sfr1 complex, but neither Swi5 nor Sfr1 alone, physically interacts with Rad51 and stimulates Rad51-mediated homologous DNA pairing. This stimulatory effect stems from the stabilization of the Rad51–ssDNA presynaptic filament. Moreover, we provide evidence that the RSfp (rodent Sfr1 proline rich) motif in Sfr1 serves as a negative regulatory element. These results thus reveal an evolutionarily conserved function in the Swi5–Sfr1 complex and furnish valuable information as to the regulatory role of the RSfp motif that is specific to the mammalian Sfr1 orthologs.

INTRODUCTION

Homologous recombination (HR) eliminates deleterious chromosomal lesions, such as the DNA double-strand break (DSB), and mediates the restart of stalled or collapsed DNA replication forks (1–5). As such, HR is indispensable for the maintenance of genome integrity and for tumor suppression (6–8). In HR that is induced by DSB formation, the nucleolytic processing of the break ends generates 3′-ssDNA tails. Polymerization of protomers of the Rad51 recombinase onto the ssDNA leads to the assembly of a helical Rad51 filament, often referred to as the presynaptic filament. The presynaptic filament engages duplex DNA, searches for homology in the duplex, and upon homology location, catalyzes the invasion of the duplex molecule to form a displacement loop, or D-loop. The D-loop structure can be resolved by one of several pathways to generate different recombinant types (9–12).

Genetic screening in the fission yeast has identified Swi5 as a factor needed for HR-mediated mating type switching. Importantly, *swi5* null cells exhibit sensitivity to DNA damaging agents such as methyl methane sulfonate (MMS) and γ-irradiation (13–16). The DNA damage sensitivity of the *swi5* mutant is milder than that of the *rad51* mutant, and the *swi5 rad51* double mutant is as sensitive as the *rad51* single mutant. The epistatic relationship of *swi5* and *rad51* suggests that Swi5 protein functions in Rad51-mediated HR (13,14). As revealed in yeast two-hybrid and co-immunoprecipitation experiments, Swi5 interacts with Sfr1 (Swi five-dependent recombination repair protein 1). The *swi5* and *sfr1* mutants exhibit the same DNA repair phenotype, and the *swi5 sfr1* double mutant is no more sensitive to DNA damage as the single mutants, indicative of epistasis (13,14,16).

The genes that encode mouse and human Swi5 and Sfr1 proteins have been characterized recently (17,18).

*To whom correspondence should be addressed. Tel: +886 2 23665573; Fax: +886 2 23635038; Email: peterhchi@ntu.edu.tw
Present addresses:
Myun Hwa Dunlop, Department of Cell Biology, Yale University School of Medicine, 333 Cedar St, New Haven, CT 06520, USA.
Yufuko Akamatsu, National Institute of Genetics, Sokendai, 1111 Yata, Mishima, Shizuoka 411-8540, Japan.

The authors wish it to be known that, in their opinion, the first two authors should be regarded as joint First Authors.

Consistent with the genetic observations in *Schizosaccharomyces pombe*, Swi5 or Sfr1 knockout in mouse embryonic stem cells or knockdown in human cell lines engenders sensitivity to DNA damaging agents such as etoposide and X-ray. Moreover, genetic analyses have provided evidence that Swi5 and Sfr1 function in Rad51-dependent HR and recombinational DNA repair (17,18). Like their *S. pombe* counterparts, the mouse and human Swi5 and Sfr1 proteins form a complex (17,18).

The heterodimeric *S. pombe* Swi5–Sfr1 complex binds DNA and physically interacts with Rad51. Importantly, *S. pombe* Swi5–Sfr1 enhances the Rad51-mediated homologous DNA pairing and strand exchange reaction (19,20), and it does so by exerting a stabilizing effect on the Rad51 presynaptic filament (20). Here, we present results from our biophysical and biochemical analyses showing that the mouse Swi5 and Sfr1 proteins also form a heterodimeric complex capable of enhancing the recombinase activity of Rad51 via presynaptic filament stabilization. Surprisingly, the mouse Swi5–Sfr1 complex is devoid of a DNA-binding activity. Our results thus establish an evolutionarily conserved HR role of the Swi5–Sfr1 complex in Rad51 presynaptic filament maintenance but reveal an important difference of the mouse complex from its yeast counterpart. Interestingly, our results suggest that the RSfp motif, unique to mammalian Sfr1 orthologs, acts as a negative regulatory element.

MATERIALS AND METHODS

DNA substrates

All the oligonucleotides used were purified from a 10% polyacrylamide gel by electro-elution and filter-dialyzed in a Centricon-10 concentrator (Millipore) at 4°C into TE buffer (10 mM Tris–HCl pH 8.0, and 0.5 mM EDTA). For the homologous DNA pairing assay, the 80-mer Oligo 1: 5′-TTATGTTCATTTTTTATATCCTTTACTT TATTTTCTCTGTTTATTCATTTACTTATTTTGTAT TATCCTTATCTTATTTA was used for assembling the presynaptic filament. To prepare the target duplex 40-mer dsDNA, Oligo 2: 5′-TAATACAAAATAAGTAAATGA ATAAACAGAGAAAATAAAG was 5′-end-labeled with polynucleotide kinase (New England Biolabs) and [γ-^{32}P] adenosine triphosphate (ATP) (PerkinElmer). Following the removal of the unincorporated nucleotide with a Spin 6 column (Bio-Rad), the radiolabeled oligonucleotide was annealed to its exact complement (Oligo 3), by heating the mixture of the two oligonucleotides at 85°C for 10 min and slow cooling to 23°C. The resulting duplex was purified from a 10% polyacrylamide gel, as above.

Plasmids

Swi5, Sfr1 and Swi5–Sfr1 expression plasmids

The mouse *Swi5* cDNA was inserted into the NdeI and BamHI site of pET15b (Novagen) and the mouse *Sfr1* cDNA was inserted into the NcoI and BamHI sites of the pRSFDuet vector (Novagen) to add a $(His)_6$ tag to the amino-terminus of the two proteins. For the co-expression of Swi5 and Sfr1, the *Swi5* cDNA was inserted into the NdeI and EcoRV sites of the pRSFDuet vector that harbors the $(His)_6$-tagged *Sfr1* gene.

Swi5–dN104Sfr1 expression plasmid

The *dN104Sfr1* gene, which lacks the first 104 codons of *Sfr1* was prepared by PCR and then inserted into the NcoI and BamHI sites of the pRSFDuet vector that harbors the *Swi5* gene. This cloning step also added a $(His)_6$ tag to the amino-terminus of the dN104Sfr1 protein.

Rad51 expression plasmid

The mouse Rad51 cDNA was inserted into the BamHI site of pRSFDuet and pET51b vectors (Novagen) to add a $(His)_6$ tag and Strep tag to the amino-terminus of the protein, respectively.

Protein expression and purification

Detailed protein expression and purification procedures for Swi5, Sfr1, Swi5–Sfr1, Swi5–dN104Sfr1 and Rad51 are described in Supplementary Materials and Methods.

Exonuclease I protection assay

$(His)_6$-tagged Rad51 (1.3 μM) was incubated with 5′-^{32}P-labeled 80-mer Oligo 1 ssDNA (3 μM nucleotides) in 18 μl buffer A (35 mM Tris–HCl pH 7.5, 1 mM DTT, 2.5 mM $MgCl_2$, 0.1 mM ATP, 25 mM KCl and 100 ng/μl BSA) at 37°C for 5 min. Following the incorporation of the indicated amount of Swi5, Sfr1, Swi5–Sfr1 or Swi5–dN104Sfr1 and a 5-min incubation, exonuclease I (1.5 units; New England Biolabs) was added to the reaction mixture (20 μl final volume). After 10 min of incubation at 37°C, a 10 μl aliquot was removed and mixed with 2.5 μl of 60 mM EDTA, 0.5% SDS and proteinase K (1 mg/ml) and incubated at 37°C for 10 min. The reaction mixtures were resolved in 10% polyacrylamide gels in TBE buffer (89 mM Tris, 89 mM borate, and 2 mM EDTA pH 8.0) and the DNA species were quantified by phosphorimaging analysis.

DNA strand exchange reaction

Unless stated otherwise, all the reaction steps were carried out at 37°C. The 80-mer Oligo 1 (4.8 μM nucleotides) was incubated with $(His)_6$-tagged Rad51 (1.6 μM) in 10.5 μl buffer A containing 1 mM ATP for 5 min. The indicated amount of Swi5, Sfr1, Swi5–Sfr1 or Swi5–dN104Sfr1 complex was then added in 1 μl, followed by a 5-min incubation. The reaction was initiated by adding homologous ^{32}P-labeled 40-mer duplex (2.4 μM base pairs) to 12.5 μl of final volume. At the indicated times, a 5 μl aliquot was removed and mixed with an equal volume of 1% SDS containing proteinase K (1 mg/ml) and incubated at 37°C for 10 min. The samples were analyzed by gel electrophoresis and phosphorimaging analysis, as above.

Isothermal titration calorimetry

The interaction between Swi5 and Sfr1 was analyzed by a microcalorimeter (iTC200 from GE Healthcare). Before performing the experiments, the proteins were dialyzed against the buffer (25 mM Tris–HCl pH 7.5, 100 mM KCl) used. Sfr1 at 11 μM was titrated with 18–20

(2 μl each) additions of 148 μM Swi5. Each injection lasted 4 and 180 s were allowed for each reaction to reach completion. The mixture was continuously stirred at 1000 rpm for heat dissipation. The heat released was plotted against the ratio of Swi5 to Sfr1.

Analytical ultracentrifugation

The assembly state and molar mass of Swi5–Sfr1 were determined using analytical ultracentrifugation (AUC) in a Beckman–Coulter XL-A Analytical Ultracentrifuge. The protein was first dialyzed exhaustively against the buffer (50 mM Tris–HCl pH 7.5, 100 mM KCl) used and then diluted to a concentration of 1.2 mg/ml for centrifugation. Swi5–Sfr1 was loaded on a six-hole charcoal-filled Epon centerpiece and sedimentation experiments were performed at 7500, 12 500 and 22 000 rpm at 4°C until equilibrium was reached. The equilibrium scans were analyzed with the Beckman–Coulter software using the single ideal species model (21). Sedimentation velocity were determined at 20°C and 40 000 rpm. Swi5–Sfr1 was loaded onto standard double sector cells with an Epon charcoal-filled centerpiece. The experimental data were analyzed by the Sedfit program (version 12.1). The gray scale of residual bitmap showed a high quality fit. After the ultracentrifugation experiments, the protein samples were visually checked for clarity and no indication of precipitation was found.

Affinity pulldowns

Strep-tagged Rad51 (3.2 μg) was incubated with either 5 μg Swi5–Sfr1 containing a $(His)_6$ tag in Sfr1's amino-terminus, 1.5 μg $(His)_6$–Swi5, 3.3 μg $(His)_6$–Sfr1 or 4 μg Swi5–dN104Sfr1 with a $(His)_6$ tag in dN104Sfr1's amino-terminus in 30 μl buffer B (25 mM Tris–HCl pH 7.5, 10% glycerol, 0.01% Igepal, 100 mM KCl, 1 mM 2-mercaptoethanol and 5 mM imidazole) for 30 min at 4°C. After being mixed with 10 μl of Talon beads for 30 min at 4°C to capture the $(His)_6$-tagged protein and associated Rad51, the beads were washed three times with 30 μl buffer B and then treated with 25 μl 2% SDS to elute proteins. The supernatant, last wash and SDS eluate, 10 μl each, were analyzed by SDS–PAGE (polyacrylamide gel electrophoresis).

RESULTS

Mammalian Swi5, Sfr1 and the Swi5–Sfr1 complex

Swi5 and *Sfr1* cDNAs isolated from mouse embryonic stem cells (17) were used to express the encoded proteins individually in *Escherichia coli* (Figure 1A, lanes 2 and 3), and procedures were developed for their purification to near homogeneity. Mouse Swi5 and Sfr1 and their human counterparts physically interact and are required for their mutual stability (17,18). Indeed, when co-expressed in *E. coli*, Swi5 and Sfr1 co-purified through several chromatographic steps, including affinity chromatography specific for the $(His)_6$ tag on Sfr1. Purified Swi5–Sfr1 complex contained stoichiometric amounts of the two proteins (Figure 1A, lane 1). Several independent preparations of the Swi5–Sfr1 complex and individually purified Swi5 and Sfr1 proteins gave the same results in all the biochemical experiments described below.

Biophysical characterization of the Swi5–Sfr1 complex

We conducted isothermal titration calorimetrical (ITC) analysis to determine the stoichiometric ratio of Swi5 and Sfr1 in the protein complex. Direct titrations of Sfr1 into a solution of Swi5 revealed that they associate in a 1:1 stoichiomeric ratio (Figure 1B). To confirm the stoichiometry and the oligomerization status of the Swi5–Sfr1 complex, we performed AUC experiments with sedimentation equilibrium and velocity methods. In the equilibrium analysis, the concentration distribution of protein species depends only on their molecular mass. As shown in Figure 1C, the sedimentation profile of Swi5–Sfr1 revealed a molecular mass of 47.5 kDa (Figure 1C), which is very close to the calculated, combined molecular weight of 46 kDa for Swi5 and Sfr1 proteins. We note that velocity ultracentrifugation also showed an apparent ~46 kDa molecular weight of the Swi5–Sfr1 complex (Supplementary Figure S1). The biophysical analyses of Swi5–Sfr1 thus indicate a heterodimeric complex with 1:1 stoichiometry.

Swi5–Sfr1 stimulates Rad51 recombinase activity

Genetic studies have implicated Swi5 and Sfr1 in Rad51-mediated HR (13,14,17,18), and enhancement of the recombinase activity of *S. pombe* Rad51 by its cognate Swi5–Sfr1 complex has been noted (19,20). We used a homologous DNA pairing and strand exchange assay to ask whether the purified mouse Swi5–Sfr1 complex stimulates the recombinase activity of mouse Rad51. In this reaction, the ssDNA substrate is incubated with Rad51 to allow for presynaptic filament assembly and then a varying amount of Swi5–Sfr1 is incorporated. The reaction is completed by the addition of a radiolabeled homologous dsDNA molecule. After incubation, the level of the DNA strand exchange product is determined by phosphorimaging analysis after gel electrophoresis (Figure 2A). Importantly, we found that Swi5–Sfr1 enhances the Rad51-mediated reaction in a concentration- and time-dependent manner (Figure 2B and C). We note that Swi5–Sfr1 alone has no DNA strand exchange activity. Near maximal stimulatory effect occurs at 1:1 stoichiometric ratio between the Swi5–Sfr1 complex and Rad51, where 9-fold enhancement occurs (Figure 2B). Rad51 presynaptic filament assembly requires ATP (22). Accordingly, even when Swi5–Sfr1 was present, no DNA strand exchange product was seen upon the omission of ATP, or when ADP (Adenosine diphosphate) was used instead (Figure 2D). Importantly, the effect of Swi5–Sfr1 is specific for Rad51, as no enhancement of DNA strand exchange mediated by the bacterial recombinase RecA was seen even at the highest Swi5–Sfr1 concentration (Figure 2E).

Interaction of Swi5–Sfr1 with Rad51

We next examined whether Swi5–Sfr1 physically interacts with Rad51. To do so, Swi5–Sfr1 was mixed with Rad51, and Talon beads [which recognize the $(His)_6$ tag on Sfr1]

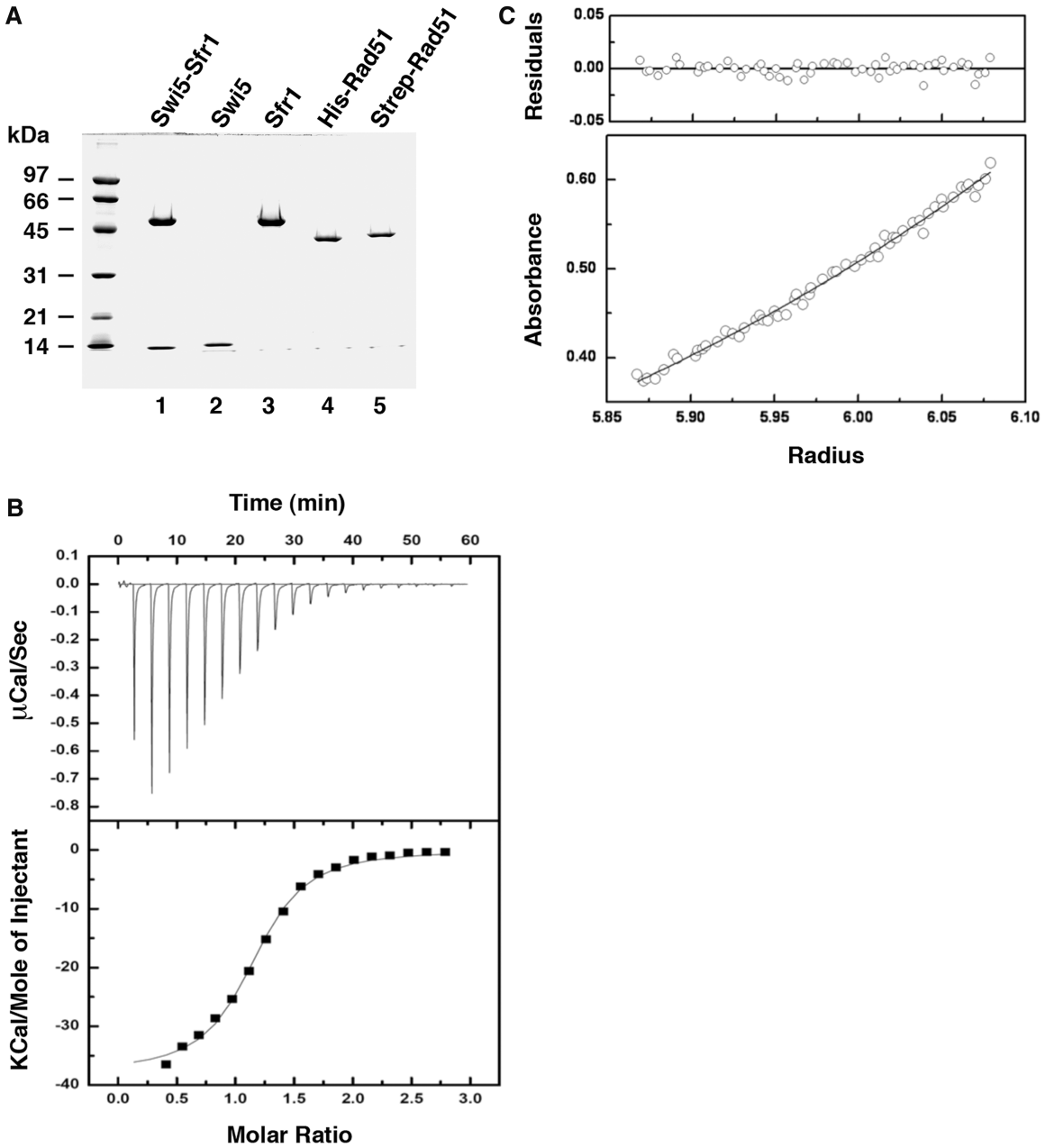

Figure 1. Biophysical properties of the Swi5–Sfr1 complex. (**A**) Purified Swi5–Sfr1 (lane 1), Swi5 (lane 2), Sfr1 (lane 3), $(His)_6$-tagged Rad51 (His-Rad51, lane 4) and Strep-tagged Rad51 (Strep-Rad51, lane 5) were resolved by 13% SDS–PAGE and stained with Coomassie Blue staining. Note that Sfr1 (36 kDa) exhibits an aberrantly slow mobility in SDS–PAGE (17). (**B**) Isothermal titration calorimetry to determine the stoichiometric ratio of Swi5 to Sfr1. The top plot summarizes the programmed sequence of 17 injections of Swi5 into the chamber that contained Sfr1. The lower plot shows the integrated binding isotherm with experimental points and best fit. (**C**) Sedimentation equilibrium analysis of the Swi5–Sfr1 complex. The average molecular mass was estimated to be 47.5 kDa. The upper part of the figure shows the residual difference between experimental and fitted values by standard deviation.

were used to isolate Swi5–Sfr1 and any associated Rad51. *Escherichia coli* RecA was included in the pull-down assay to address the specificity of protein complex formation. As shown in Figure 3A, Rad51, but not RecA, associated with Swi5–Sfr1 avidly. Importantly, no interaction of Swi5 or Sfr1 [both tagged with the $(His)_6$ epitope] with Rad51 occurred (Figure 3B). Consistent with this observation, over a wide protein concentration range, neither Swi5 (Figure 4A) nor Sfr1 (Figure 4B) had any stimulatory effect on Rad51 activity. Taken together, the results indicated that Swi5–Sfr1 interacts with Rad51, but that this interaction is contingent upon complex formation between Swi5 and Sfr1. Moreover, the DNA strand exchange results correlate with those from the affinity pull-down experiments in showing that Swi5–Sfr1, but not Swi5 or Sfr1, stimulates the recombinase function of Rad51.

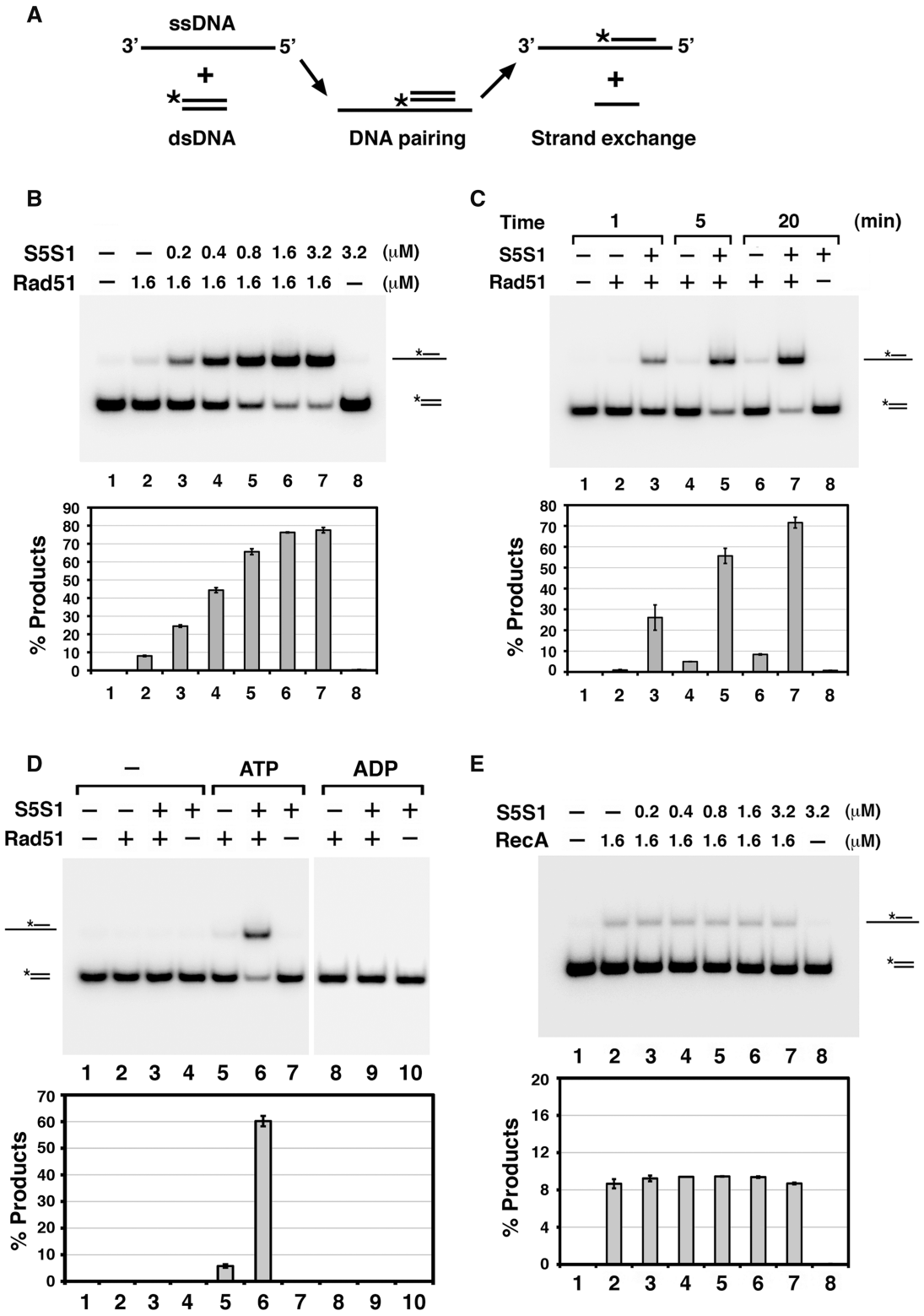

Figure 2. Promotion of Rad51-mediated DNA strand exchange by Swi5–Sfr1. (**A**) Schematic of the DNA strand exchange assay. The radiolabeled substrate and product are visualized and quantified by phosphorimaging analysis after PAGE. The asterisk denotes the ^{32}P label. (**B**) DNA strand exchange reactions with the indicated concentrations of Rad51 and Swi5–Sfr1. The incubation time was 20 min. (**C**) Time kinetics of DNA strand exchange mediated by Rad51 alone (1.6 μM) or with Swi5–Sfr1 (1.6 μM). The results were graphed. (**D**) DNA strand exchange by Rad51 (1.6 μM) with or without Swi5–Sfr1 (1.6 μM) was examined. Either ATP or ADP was included in the reaction, as indicated. The incubation time was 10 min. (**E**) The DNA strand exchange activity of RecA was examined and with or without the indicated concentration of Swi5–Sfr1. The incubation time was 20 min. (B–E) Error bars represent the standard deviation (±SD) calculated based on at least three independent experiments. Symbol: S5S1, Swi5–Sfr1.

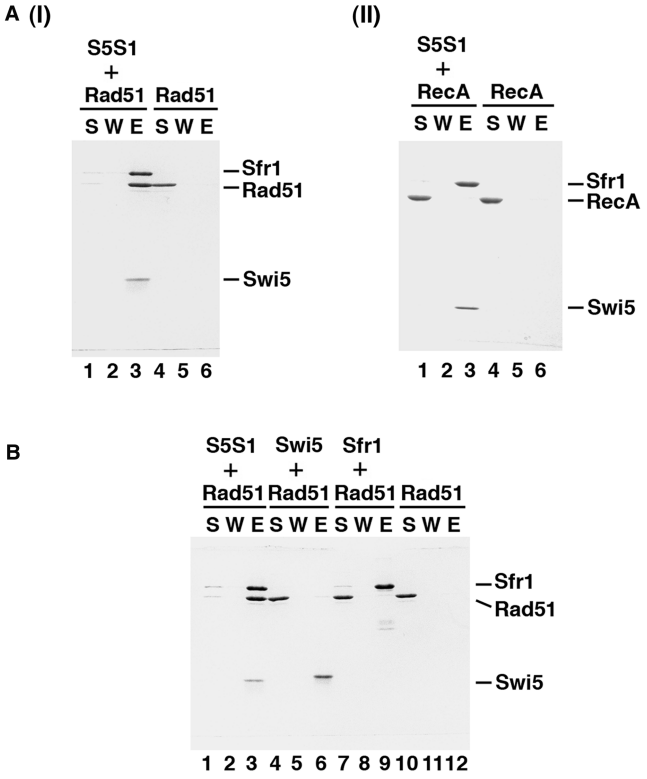

Figure 3. Swi5–Sfr1 complex but not Swi5 or Sfr1 physically interacts with Rad51. (**A**) For affinity pulldown, purified Swi5–Sfr1 (S5S1) with a $(His)_6$ tag on Sfr1 was incubated with either Rad51 (panel I) or RecA (panel II), and the reaction mixtures were mixed with Talon beads to capture protein complex through the $(His)_6$ tag. The supernatant (S), wash (W) and SDS elute (E) from the pull-down reaction were analyzed by 13% SDS–PAGE with Coomassie Blue staining. Rad51 and RecA alone were included as controls. (**B**) Purified $(His)_6$-tagged Swi5, Sfr1 and Swi5–Sfr1 were incubated with Rad51 to examine their interaction. Symbol: S5S1, Swi5–Sfr1.

Stabilization of the Rad51 presynaptic filament by the Swi5–Sfr1 complex

Cytological studies have furnished evidence that Swi5–Sfr1 affects the assembly or maintenance of the Rad51 presynaptic filament in human cells (18). Consistent with this finding, the *S. pombe* Swi5–Sfr1 complex has been found to stabilize the Rad51 presynaptic filament (13,14). To ask whether mouse Swi5–Sfr1 possesses a presynaptic filament stabilization function, we monitored the susceptibility of a 5′-^{32}P-labeled ssDNA to *E. coli* exonuclease I (a 3′- to 5′-exonuclease) in the presence of only Rad51 or the combination of Rad51 and Swi5–Sfr1 in reactions that contained ATP as the nucleotide cofactor for presynaptic filament assembly (see schematic in Figure 5A). Importantly, the susceptibility of the ssDNA to exonuclease I was greatly attenuated by the inclusion of Swi5–Sfr1, with maximal protection being observed at a Swi5–Sfr1 to Rad51 stoichiometric ratio of 1:1 (Figure 5B). Control experiments showed that (i) in the absence of Rad51, Swi5–Sfr1 is devoid of the ability to protect ssDNA against exonuclease action (Figure 5B), (ii) neither Swi5 nor Sfr1 has any protective effect (Figure 5C) and (iii) Swi5–Sfr1 exerts no protective effect when used in combination with RecA (Supplementary Figure S2).

In addition to exonuclease I protection, we employed a DNA topology change assay to examine the effect of Swi5–Sfr1 on the stability of the Rad51 presynaptic filament. In this assay, topologically relaxed duplex DNA is added to trap Rad51 molecules that have dissociated from ssDNA. Since binding of Rad51 molecules induces a topological change in the duplex DNA upon the addition of calf thymus topoisomerase I (23), this procedure provides a convenient means to monitor Rad51 presynaptic filament turnover (Supplementary Figure S3A). Importantly, the results from this assay provided independent verification for the presynaptic

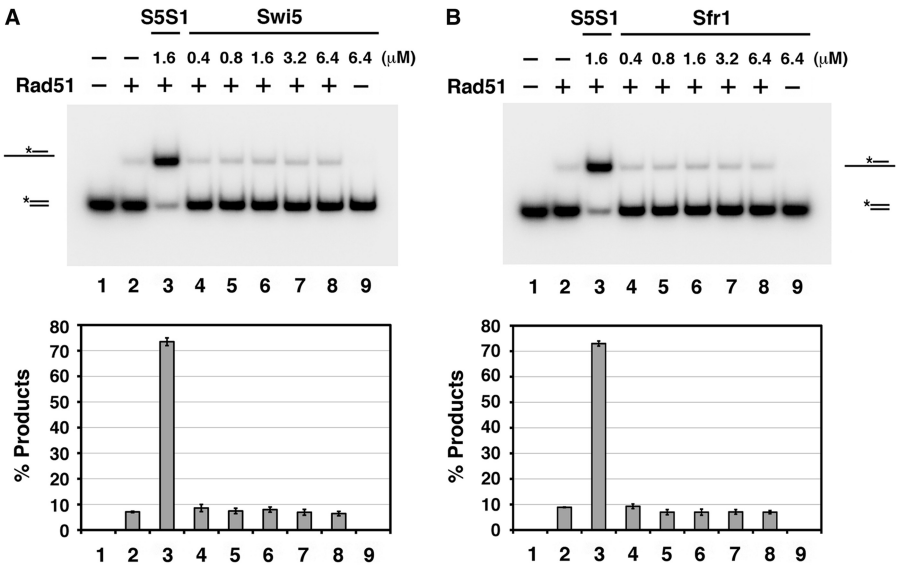

Figure 4. Enhancement of Rad51-mediated DNA strand exchange by Swi5–Sfr1. (**A**) and (**B**) DNA strand exchange reactions containing Rad51 (1.6 μM) and the indicated amount of Swi5, Sfr1 or Swi5–Sfr1. The incubation time was 20 min. The results were graphed. Error bars represent the standard deviation (± SD) calculated based on at least three independent experiments. Symbol: S5S1, Swi5–Sfr1.

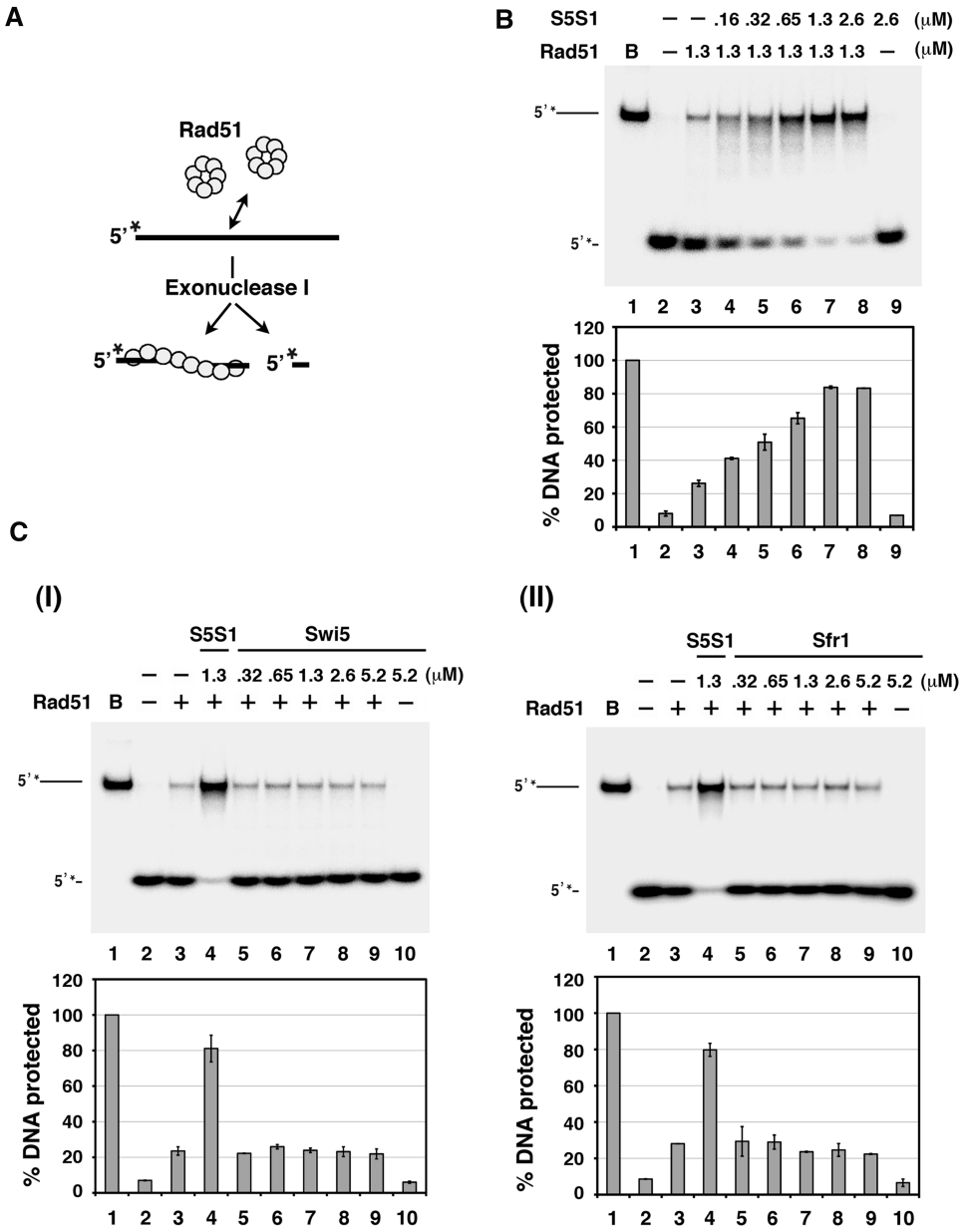

Figure 5. Stabilization of the Rad51 presynaptic filament by Swi5–Sfr1. (**A**) Schematic of the exonuclease I protection assay for examining presynaptic filament stability. The Rad51 presynaptic filament harboring 5′-^{32}P-labeled DNA is incubated with exonuclease I. The radiolabeled DNA and product are visualized and quantified by phosphorimaging analysis after PAGE. The ^{32}P label is denoted by the asterisk. (**B**) The Rad51 presynaptic filament was treated with exonuclease I in the absence or presence of the indicated concentration of Swi5–Sfr1. The results were graphed. (**C**) The Rad51 presynaptic filament was treated with exonuclease I in the absence or presence of the indicated concentration of Swi5 (panel I), Sfr1 (panel II) or Swi5–Sfr1. The results were graphed. (B and C) Error bars represent the standard deviation (±SD) calculated based on at least three independent experiments. Symbol: S5S1, Swi5–Sfr1.

filament stabilization function of the Swi5–Sfr1 complex (Supplementary Figure S3B). Again, neither Swi5 nor Sfr1 alone could stabilize the presynaptic filament (data not shown), and Swi5–Sfr1 alone is unable to induce a topological change in the DNA (Supplementary Figure S3B).

A stabilized Rad51 presynaptic filament is unresponsive to Swi5–Sfr1

If presynaptic filament stabilization is the sole function of Swi5–Sfr1, then a presynaptic filament that is rendered stable by another means should be unresponsive to the Swi5–Sfr1 complex. Since the dissociation of Rad51 from ssDNA is intimately linked to ATP hydrolysis (3,12,23–28), one can assemble a stable Rad51 presynaptic filament by using AMP-PNP (Adenylyl-imidodiphosphate), a non-hydrolyzable ATP analog, as nucleotide cofactor. Importantly, little or no significant enhancement of the Rad51-mediated DNA strand exchange reaction occurred when AMP-PNP was used in lieu of ATP (Figure 6A). The inclusion of calcium ion has been shown to markedly slow the turnover of

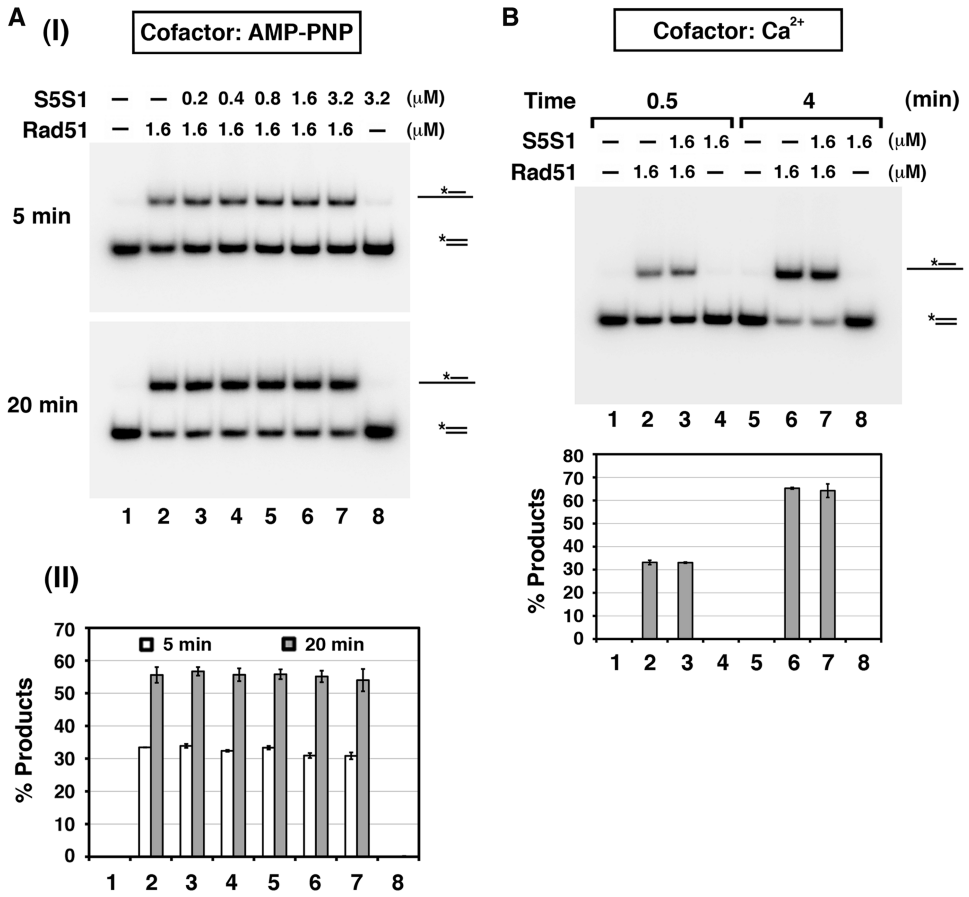

Figure 6. Presynaptic filament stabilization by AMP-PNP or Ca^{2+} alleviates dependence on Swi5–Sfr1. (**A**) DNA strand exchange was conducted using AMP-PNP as the nucleotide cofactor. The results were graphed. (**B**) DNA strand exchange was conducted in the presence of Ca^{2+}. The results were graphed. (A and B) Error bars represent the standard deviation (±SD) calculated based on at least three independent experiments. Symbol: S5S1, Swi5–Sfr1.

Rad51 protomers from ssDNA even when ATP is used (24). As shown in Figure 6B, the addition of Swi5–Sfr1 has no significant stimulatory effect on Rad51-mediated DNA strand exchange in the presence of calcium ion. In summary, the results presented here provide evidence that Swi5–Sfr1 enhances Rad51 recombinase function primarily, or solely, via presynaptic filament stabilization.

The RSfp motif in Sfr1 is inhibitory to Swi5–Sfr1 function

Mouse Sfr1 harbors a proline-rich motif at its N-terminus, named the RSfp (rodent Sfr1 proline rich) motif [Figure 7A; (17)]. The RSfp motif is found in mammalian species only (17). To address the functional role of this motif, we constructed the Sfr1dN104 mutant that deletes the N-terminal 104 amino acid residues encompassing the tandem RSfp repeats (Figure 7A). When co-expressed with Swi5 in *E. coli*, dN104Sfr1 forms a stable complex with the former, which is in agreement with a previous study (17). The mutant complex could be purified to near homogeneity using the same chromatographic procedure for the wild-type counterpart (Figure 7B). We employed affinity pulldown through the $(His)_6$ tag on the mutant Sfr1 to examine whether the RSfp motif is required for Rad51 interaction. As shown in Figure 7C, Swi5–dN104Sfr1 bound Rad51 just as avidly as wild-type Swi5–Sfr1 (Figure 7C) and, as expected, had no affinity for RecA (data not shown). The above results thus revealed that the RSfp motif in Sfr1 is dispensable for complex formation with Swi5 and for the interaction of Swi5–Sfr1 with Rad51.

We next wished to ascertain whether Swi5–dN104Sfr1 is proficient in functional interactions with Rad51. The analysis of Swi5–dN104Sfr1 in the Rad51-mediated DNA strand exchange reaction indicated that the mutant complex stimulates DNA strand exchange efficiency in the presence of ATP (Figure 7D). Unexpectedly, the mutant complex is significantly more adept at Rad51 enhancement than the wild-type counterpart. For instance, at a stoichiomteric ratio of Swi5–Sfr1:Rad51 of 1:8, while the wild-type complex enhanced the strand exchange reaction by 2.5-fold, the mutant complex exerted more than a 7-fold stimulation (compare Figure 2B, lanes 2 and 3 and Figure 7D, lanes 2 and 5). Likewise, in the exonuclease I-based and DNA topology change assays to probe for the stability of the Rad51 presynaptic filament, the Swi5–dN104Sfr1 mutant complex possesses a much more robust presynaptic

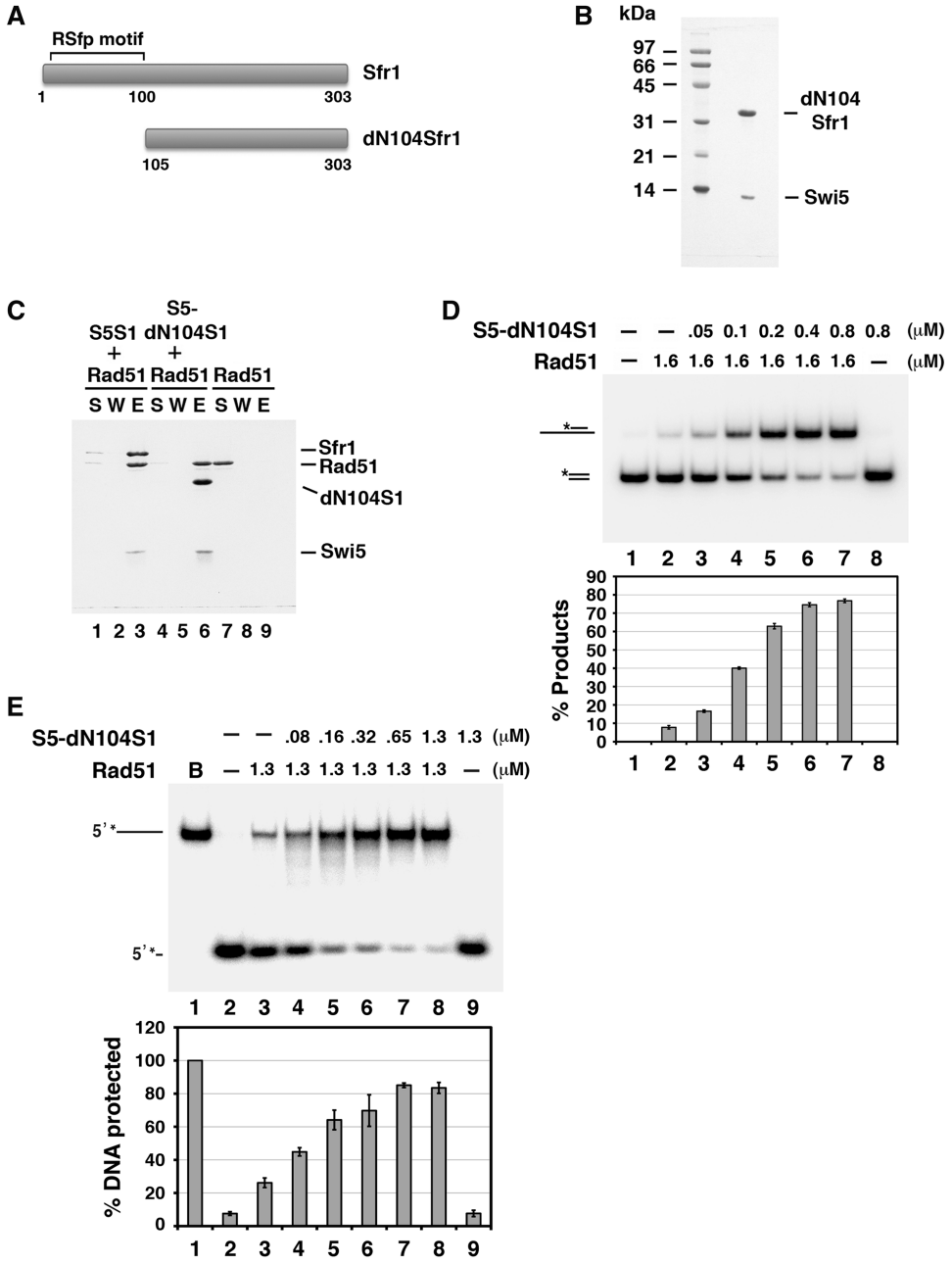

Figure 7. Functional significance of the RSfp motif in Sfr1. (**A**) Sfr1 (303 residues) harbors a RSfp motif in its N-terminus. This motif is deleted in the dN104Sfr1 mutant. (**B**) Purified Swi5–dN104Sfr1 complex (1.5 μg) was subjected to 13% SDS–PAGE and Coomassie Blue staining. (**C**) Purified Swi5–dN104Sfr1 mutant complex was tested for Rad51 interaction by affinity pulldown through the $(His)_6$ tag on dN104Sfr1. The supernatant (S), wash (W) and SDS elute (E) from the pull-down reaction were analyzed by 13% SDS–PAGE with Coomassie Blue staining. (**D**) DNA strand exchange was conducted with the indicated concentration of Swi5–dN104Sfr1. The results were graphed. (**E**) The stability of the Rad51 presynaptic filament was tested by the exonuclease I assay with the indicated concentration of Swi5–dN104Sfr1. The results were graphed. (D and E) Error bars represent the standard deviation (±SD) calculated based on at least three independent experiments. Symbols: S5S1, Swi5–Sfr1; S5-dN104S1, Swi5–dN104Sfr1.

filament stabilization effect than does the wild-type complex (compare Figure 5B and Figure 7E; Supplementary Figures S3B and S4). In summary, the results show that the RSfp motif is not only dispensable for functional interactions with Rad51, but it seems to attenuate the Rad51 presynaptic filament stabilization function.

DISCUSSION

Physical and functional interactions of the mammalian Swi5–Sfr1 complex with Rad51

Previous genetic and biochemical studies (17,18) have provided evidence that mouse and human Swi5 and Sfr1 proteins form a complex that functions in Rad51-mediated

HR. We have developed procedures for the expression and purification of Swi5, Sfr1 and the Swi5–Sfr1 complex, and have furnished several lines of biophysical evidence pointing to a heterodimeric complex with 1:1 stoichiometry for Swi5 and Sfr1. Importantly, our results have shown that Swi5–Sfr1, but not Swi5 or Sfr1, physically interacts with Rad51 and stimulates Rad51-mediated DNA strand exchange. Interestingly, this stimulatory function of Swi5–Sfr1 is not seen under conditions wherein the Rad51 presynaptic filament is rendered stable by the use of a non-hydrolyzable ATP analog or the inclusion of calcium ion in the DNA strand exchange reaction. Taken together, the results provided tantalizing evidence that the primary function of Swi5–Sfr1 is to maintain the Rad51 presynaptic filament in a stable form. Indeed, using two separate biochemical assays, we have shown that amounts of Swi5–Sfr1 stoichiometric to that of Rad51 exert a marked stabilizing effect on the presynaptic filament. We note that Swi5–Sfr1, under conditions of the DNA strand exchange reaction, does not bind either ssDNA or dsDNA (Supplementary Figure S5).

A recently published study reported that depletion of either *SWI5* or *SFR1* in human cells does not affect the resection of DSB ends to generate the HR substrate, but, rather, impairs the formation of DNA damage-induced nuclear Rad51 foci. These biological data thus implicate Swi5–Sfr1 in the assembly or maintenance of the Rad51 presynaptic filaments in human cells (18). Our biochemical data now provide direct evidence that the Swi5–Sfr1 complex functions in the presynaptic phase of the HR reaction, specifically, by stabilizing the Rad51 presynaptic filament.

Comparison of the mouse Swi5–Sfr1 complex with its *Schizosaccharomyces pombe* and *Saccharomyces cerevisiae* orthologs

There are clear parallels between the mouse Swi5–Sfr1 complex and its *S. pombe* ortholog (19,20). Most notably, both protein complexes are heterodimeric and both have been shown to stabilize the Rad51 presynaptic filament [(29); this work]. Like *S. pombe* Swi5–Sfr1 (19), the mouse ortholog also elevates the DNA-dependent ATPase activity of Rad51 (our unpublished data). Moreover, both *S. pombe* Swi5–Sfr1 and mouse Swi5–Sfr1 interact with Rad51 (13,19; this work), we have presented evidence herein that complex formation between mouse Swi5 and Sfr1 is a prerequisite for Rad51 interaction.

Saccharomyces cerevisiae Mei5 and Sae3 proteins are the respective orthologs of Sfr1 and Swi5, and these proteins also form a stable complex that possesses a DNA-binding activity (30,31). However, the expression of the Mei5–Sae3 complex is restricted solely to meiosis (32,33), where it has been suggested to function with the meiotic recombinase Dmc1 [(30,32,33); see next section]. Even though Mei5–Sae3 appears to physically interact with Rad51 through Mei5, no enhancement of the Rad51 recombinase activity by this protein complex has been seen (31).

Possible meiotic role of the Swi5–Sfr1 complex

Genetic studies in *S. pombe* and *S. cerevisiae* have provided compelling evidence for a role of the Swi5–Sfr1 and Mei5–Sae3 complexes in meiotic HR. Yeast strains that harbor mutations in these protein complexes sporulate poorly and exhibit low spore viability, defects that stem from impaired HR, particularly of the crossover type that is needed for chromosome disjunction in meiosis I (15,32–35). Interestingly, Mei5–Sae3 and Dmc1 co-localize on meiotic chromosomes as foci, and the formation of the Mei5–Sae3 foci is dependent on Dmc1 being present, and vice versa (32,33). Consistent with these findings, both the Swi5–Sfr1 and the Mei5–Sae3 complexes physically interact with Dmc1, which, as alluded above, is meiosis-specific and more adept than Rad51 in generating crossover recombinants between homologous chromosome pairs. Moreover, Mei5–Sae3 helps overcome the inhibitory effect of RPA (Replication protein A), the evolutionarily conserved single-strand DNA-binding protein, on Dmc1-mediated DNA strand exchange. This effect of Mei5–Sae3 stems from its ability to promote the assembly of the Dmc1 presynaptic filament on ssDNA coated by RPA (30), thus qualifying Mei5–Sae3 as a Dmc1-specific recombination mediator (12). Even though *S. pombe* Swi5–Sfr1 clearly stimulates Dmc1-mediated DNA strand exchange, it is not clear whether it also possesses a recombination mediator activity capable of overcoming the inhibitory effect of RPA on presynaptic filament assembly (19).

Given the above findings on *S. cerevisiae* Mei5–Sae3 and *S. pombe* Swi5–Sfr1, it seems likely that the mammalian Swi5–Sfr1 complex also plays a role in meiotic HR by facilitating Dmc1-mediated DNA strand exchange (15,16,19). The availability of highly purified mouse Swi5–Sfr1 (this work) will be valuable for testing this premise.

The regulatory role of the RSfp motif in Sfr1

The RSfp motif does not exist in the *S. cerevisiae* or *S. pombe* ortholog. Importantly, we have shown that a mouse Sfr1 mutant lacking the entire RSfp motif, when complexed with Swi5, not only retains all the functional attributes of the wild-type protein, but it actually acquires an enhanced capability to stabilize the Rad51 presynaptic filament and to promote Rad51-mediated DNA strand exchange. Our results thus provide evidence that the HR activity of the mammalian Swi5–Sfr1 complex is negatively regulated by the RSfp motif in Sfr1, and they also suggest the intriguing possibility of a mechanism that alleviates the suppressive effect of this motif to allow efficient HR to proceed upon the occurrence DNA damage or during meiosis. Such a hypothetical mechanism could entail a post-translational modification event or a novel HR factor. The protein purification procedures and biochemical systems documented herein should facilitate future efforts directed at delineating the basis for the negative regulatory effect of the RSfp motif.

Other Rad51 accessory factors with a presynaptic filament maintenance role

Rad54 and Hop2–Mnd1 are accessory factors of Rad51. Both Rad54 and Hop2–Mnd1 stabilize the Rad51 presynaptic filament (36–38), but they differ from Swi5–Sfr1 in serving additional functions. Hop2–Mnd1

has a dsDNA-binding activity and enhances the ability of the Rad51 filament to capture dsDNA (36). Rad54, on the other hand, possesses a DNA translocase activity that is fueled by ATP hydrolysis (38). This activity allows Rad54 to facilitate homologous DNA pairing via supercoiling of the dsDNA partner (38) and to remove Rad51 from dsDNA (39). The latter attribute of Rad54 helps prevent the non-specific association of Rad51 with bulk chromatin (40) and also helps free the primer end in the D-loop structure to initiate repair DNA synthesis (39). Future studies will determine whether Swi5–Sfr1 acts in a synergistic or additive fashion with these other HR factors in presynaptic filament stabilization.

SUPPLEMENTARY DATA

Supplementary Data are available at NAR Online: Supplementary Figures 1–5, Supplementary Materials and Methods and Supplementary Reference [23].

FUNDING

The Taiwan National Science Council [NSC 99-2311-B-002-012 and NSC 100-2311-B-002-009 to P.C.]; US National Institutes of Health [RO1 GM54668 to M.J. and RO1 ES015252 to P.S.]. Funding for open access charge: The Taiwan National Science Council [NSC 100-2311-B-002-009].

Conflict of interest statement. None declared.

REFERENCES

1. Flores-Rozas,H. and Kolodner,R.D. (2000) Links between replication, recombination and genome instability in eukaryotes. *Trends Biochem. Sci.*, **25**, 196–200.
2. Haber,J.E. (1999) DNA recombination: the replication connection. *Trends Biochem. Sci.*, **24**, 271–275.
3. Heyer,W.D., Ehmsen,K.T. and Liu,J. (2010) Regulation of homologous recombination in eukaryotes. *Annu. Rev. Genet.*, **44**, 113–139.
4. Klein,H.L. and Kreuzer,K.N. (2002) Replication, recombination, and repair: going for the gold. *Mol. Cell*, **9**, 471–480.
5. Petermann,E. and Helleday,T. (2010) Pathways of mammalian replication fork restart. *Nat. Rev. Mol. Cell Biol.*, **11**, 683–687.
6. Hartlerode,A.J. and Scully,R. (2009) Mechanisms of double-strand break repair in somatic mammalian cells. *Biochem. J.*, **423**, 157–168.
7. Klein,H.L. (2008) The consequences of Rad51 overexpression for normal and tumor cells. *DNA Repair*, **7**, 686–693.
8. Moynahan,M.E. and Jasin,M. (2010) Mitotic homologous recombination maintains genomic stability and suppresses tumorigenesis. *Nat. Rev. Mol. Cell Biol.*, **11**, 196–207.
9. Holthausen,J.T., Wyman,C. and Kanaar,R. (2010) Regulation of DNA strand exchange in homologous recombination. *DNA Repair*, **9**, 1264–1272.
10. Krogh,B.O. and Symington,L.S. (2004) Recombination proteins in yeast. *Annu. Rev. Genet.*, **38**, 233–271.
11. Lisby,M. and Rothstein,R. (2009) Choreography of recombination proteins during the DNA damage response. *DNA Repair*, **8**, 1068–1076.
12. San Filippo,J., Sung,P. and Klein,H. (2008) Mechanism of eukaryotic homologous recombination. *Annu. Rev. Biochem.*, **77**, 229–257.
13. Akamatsu,Y., Dziadkowiec,D., Ikeguchi,M., Shinagawa,H. and Iwasaki,H. (2003) Two different Swi5-containing protein complexes are involved in mating-type switching and recombination repair in fission yeast. *Proc. Natl Acad. Sci. USA*, **100**, 15770–15775.
14. Akamatsu,Y., Tsutsui,Y., Morishita,T., Siddique,M.S., Kurokawa,Y., Ikeguchi,M., Yamao,F., Arcangioli,B. and Iwasaki,H. (2007) Fission yeast Swi5/Sfr1 and Rhp55/Rhp57 differentially regulate Rhp51-dependent recombination outcomes. *EMBO J.*, **26**, 1352–1362.
15. Ellermeier,C., Schmidt,H. and Smith,G.R. (2004) Swi5 acts in meiotic DNA joint molecule formation in Schizosaccharomyces pombe. *Genetics*, **168**, 1891–1898.
16. Haruta,N., Akamatsu,Y., Tsutsui,Y., Kurokawa,Y., Murayama,Y., Arcangioli,B. and Iwasaki,H. (2008) Fission yeast Swi5 protein, a novel DNA recombination mediator. *DNA Repair*, **7**, 1–9.
17. Akamatsu,Y. and Jasin,M. (2010) Role for the mammalian Swi5-Sfr1 complex in DNA strand break repair through homologous recombination. *PLoS Genet.*, **6**, e1001160.
18. Yuan,J. and Chen,J. (2011) The role of the human SWI5-MEI5 complex in homologous recombination repair. *J. Biol. Chem.*, **286**, 9888–9893.
19. Haruta,N., Kurokawa,Y., Murayama,Y., Akamatsu,Y., Unzai,S., Tsutsui,Y. and Iwasaki,H. (2006) The Swi5-Sfr1 complex stimulates Rhp51/Rad51- and Dmc1-mediated DNA strand exchange in vitro. *Nat. Struct. Mol. Biol.*, **13**, 823–830.
20. Kurokawa,Y., Murayama,Y., Haruta-Takahashi,N., Urabe,I. and Iwasaki,H. (2008) Reconstitution of DNA strand exchange mediated by Rhp51 recombinase and two mediators. *PLoS Biol.*, **6**, e88.
21. McRorie,D.K. and Voelker,P.J. (1993) Self-associating systems in the analytical ultracentrifuge. Beckman Press, Palo Alto, CA.
22. Sung,P. (1994) Catalysis of ATP-dependent homologous DNA pairing and strand exchange by yeast RAD51 protein. *Science*, **265**, 1241–1243.
23. Chi,P., Van Komen,S., Sehorn,M.G., Sigurdsson,S. and Sung,P. (2006) Roles of ATP binding and ATP hydrolysis in human Rad51 recombinase function. *DNA Repair*, **5**, 381–391.
24. Bugreev,D.V. and Mazin,A.V. (2004) Ca2+ activates human homologous recombination protein Rad51 by modulating its ATPase activity. *Proc. Natl Acad. Sci. USA*, **101**, 9988–9993.
25. Cox,M.M. (2003) The bacterial RecA protein as a motor protein. *Annu. Rev. Microbiol.*, **57**, 551–577.
26. Ristic,D., Modesti,M., van der Heijden,T., van Noort,J., Dekker,C., Kanaar,R. and Wyman,C. (2005) Human Rad51 filaments on double- and single-stranded DNA: correlating regular and irregular forms with recombination function. *Nucleic Acids Res.*, **33**, 3292–3302.
27. Robertson,R.B., Moses,D.N., Kwon,Y., Chan,P., Chi,P., Klein,H., Sung,P. and Greene,E.C. (2009) Structural transitions within human Rad51 nucleoprotein filaments. *Proc. Natl Acad. Sci. USA*, **106**, 12688–12693.
28. Robertson,R.B., Moses,D.N., Kwon,Y., Chan,P., Zhao,W., Chi,P., Klein,H., Sung,P. and Greene,E.C. (2009) Visualizing the disassembly of S. cerevisiae Rad51 nucleoprotein filaments. *J. Mol. Biol.*, **388**, 703–720.
29. Kokabu,Y., Murayama,Y., Kuwabara,N., Oroguchi,T., Hashimoto,H., Tsutsui,Y., Nozaki,N., Akashi,S., Unzai,S., Shimizu,T. *et al.* (2011) Fission yeast Swi5-Sfr1 protein complex, an activator of Rad51 recombinase, forms an extremely elongated dogleg-shaped structure. *J. Biol. Chem.*, **286**, 43569–43576.
30. Ferrari,S.R., Grubb,J. and Bishop,D.K. (2009) The Mei5-Sae3 protein complex mediates Dmc1 activity in Saccharomyces cerevisiae. *J. Biol. Chem.*, **284**, 11766–11770.
31. Say,A.F., Ledford,L.L., Sharma,D., Singh,A.K., Leung,W.K., Sehorn,H.A., Tsubouchi,H., Sung,P. and Sehorn,M.G. (2011) The budding yeast Mei5-Sae3 complex interacts with Rad51 and preferentially binds a DNA fork structure. *DNA Repair*, **10**, 586–594.
32. Hayase,A., Takagi,M., Miyazaki,T., Oshiumi,H., Shinohara,M. and Shinohara,A. (2004) A protein complex containing Mei5 and Sae3 promotes the assembly of the meiosis-specific RecA homolog Dmc1. *Cell*, **119**, 927–940.
33. Tsubouchi,H. and Roeder,G.S. (2004) The budding yeast mei5 and sae3 proteins act together with dmc1 during meiotic recombination. *Genetics*, **168**, 1219–1230.

34. Martín-Castellanos,C., Blanco,M., Rozalén,A.E., Pérez-Hidalgo,L., García,A.I., Conde,F., Mata,J., Ellermeier,C., Davis,L., San-Segundo,P. *et al.* (2005) A large-scale screen in S. pombe identifies seven novel genes required for critical meiotic events. *Curr. Biol.*, **15**, 2056–2062.
35. Young,J.A., Hyppa,R.W. and Smith,G.R. (2004) Conserved and nonconserved proteins for meiotic DNA breakage and repair in yeasts. *Genetics*, **167**, 593–605.
36. Chi,P., San Filippo,J., Sehorn,M.G., Petukhova,G.V. and Sung,P. (2007) Bipartite stimulatory action of the Hop2-Mnd1 complex on the Rad51 recombinase. *Genes Dev.*, **21**, 1747–1757.
37. Mazin,A.V., Alexeev,A.A. and Kowalczykowski,S.C. (2003) A novel function of Rad54 protein. Stabilization of the Rad51 nucleoprotein filament. *J. Biol. Chem.*, **278**, 14029–14036.
38. Van Komen,S., Petukhova,G., Sigurdsson,S., Stratton,S. and Sung,P. (2000) Superhelicity-driven homologous DNA pairing by yeast recombination factors Rad51 and Rad54. *Mol Cell*, **6**, 563–572.
39. Solinger,J.A., Kiianitsa,K. and Heyer,W.D. (2002) Rad54, a Swi2/Snf2-like recombinational repair protein, disassembles Rad51:dsDNA filaments. *Mol. Cell*, **10**, 1175–1188.
40. Shah,P.P., Zheng,X., Epshtein,A., Carey,J.N., Bishop,D.K. and Klein,H.L. (2010) Swi2/Snf2-related translocases prevent accumulation of toxic Rad51 complexes during mitotic growth. *Mol. Cell*, **39**, 862–872.